Ductility-based strength reduction factor for pulse-like and non-pulse-like ground motions

Seyyed Ebrahim Motallebi and Mehdi Poursha[1]
Faculty of Civil engineering, Tabriz University of Technology, Tabriz, Iran

Abstract
Reduction in forces, which results in inelastic deformations, is controlled by a coefficient called the strength reduction factor (R_μ). In the vicinity of active faults, ground motions are influenced by forward directivity and fling step (characterized by permanent ground displacement) effects. Previous studies have not addressed the R_μ factor considering the influence of fling step and non-pulse-like near-fault ground motion records. This paper attempts to evaluate the strength reduction factor for single-degree-of-freedom (SDOF) systems subjected to 78 pulse-like and non-pulse-like near-fault and far-fault ground motions recorded on the site classes C and D. The influence of the period of vibration, pulse period, and ductility level was studied in this paper. Moreover, in order to investigate the effect of cyclic deterioration, the modified Ibarra-Medina-Krawinkler (IMK) deterioration model with bilinear hysteretic behavior was employed. Finally, equations were proposed to obtain R_μ for different types of earthquakes. The results indicate that R_μ is strongly influenced by the period of vibration, ductility level, and cyclic deterioration. The results also show that the existing equations for calculating R_μ which are based on far-fault ground motions, can not be used for pulse-type near-fault records. Especially, for near-fault ground motions with fling step effect, applying the existing equations makes the design unsafe.

Keywords: Strength reduction factor, near-fault, fling step, forward directivity, non-pulse, far-fault, modified bilinear Ibarra-Medina-Krawinkler deterioration model.

1. Introduction

For economic causes, the current design provisions allow buildings to experience nonlinear deformations under the effect of strong ground motions. Therefore, the design lateral strengths prescribed in earthquake-resistant design provisions are, in general, lower than the lateral strength required to maintain the structure in the elastic range in the event of strong seismic ground motions. Reduction in forces or strengths which results in inelastic deformations is controlled by a coefficient called the strength reduction factor [1] .Therefore, it is important to study the parameters which influence this coefficient.
The strength reduction factor (SRF) can be described as the ratio of the elastic strength demand to the inelastic strength demand as follows:

$$R_\mu = \frac{f_y(\mu = 1)}{f_y(\mu = \mu_i)} = \frac{f_o}{f_y} = \frac{u_o}{u_y} \quad (1)$$

in which $f_y(\mu = 1)$ is the lateral yielding strength required to keep the system in the elastic state and $f_y(\mu = \mu_i)$ is the lateral yielding strength required to maintain the displacement ductility demand less or equal to a predefined target ductility demand ratio, under the same ground motion. Strength reduction factor for a single-degree-of-freedom (SDOF) system subjected to a given ground motion with a specified hysteretic behavior and a target ductility ratio, for each period of vibration, can be evaluated by an iterative method [1].

[1] Corresponding Author, Email: poursha@sut.ac.ir

One of the first studies in the field of strength reduction factor was carried out by Newmark and Hall [2]. They reported that in the long-period region, the maximum displacement of elastic and elastoplastic systems are the same (the equal displacement rule) and the SRF is equal to the target displacement ductility. Moreover, they showed that in the short-period region, the SRF is equal to $\sqrt{2\mu - 1}$. Several researchers have presented some equations by investigating the dependence of the SRF on the target ductility and the period of vibration [3-6]. Al-Sulaimani and Rossett investigated the effect of stiffness and strength degradation on the inelastic response of SDOF systems with 5% damping. They concluded that the SRF for systems that exhibit stiffness and strength degradation is less than that for the elastoplastic systems [7]. Elghadamsi and Mohraz investigated the effect of soil type on the SRF by evaluating 50 records on the alluvium site and 26 records on the rock site. They concluded that for a given ductility and period, the elastic forces are reduced more for a structure on rock than for a structure on alluvium site [8]. Peng et al. examined the effects of duration of ground motions, damping ratio and soil conditions on the SRF. According to their results, earthquakes with longer duration show a smaller SRF. Also, their study indicated that the effect of damping ratio and soil conditions is negligible [9]. Nassar and Krawinkler examined 15 earthquake records in order to study the effects of epicentral distance and stiffness degradation on the SRF for SDOF systems. The results of their study indicated that the effects of epicentral distance and stiffness degradation on the SRF can be neglected [10]. Miranda and Bertro analyzed 50 earthquakes in various site conditions in order to study the effect of normalized vibration periods. They reported that the SRFs are strongly affected by the period of vibration, the inelastic deformation and the local site conditions. Also, for soft soil sites, the evaluation of the predominant period of a seismic ground motion is very important [11]. In a study conducted by Miranda, the effect of earthquake magnitude and epicentral distance on the SRF was investigated, and they were shown to be insignificant; on the contrary, the effect of soil conditions in soft soil sites was considerable [1]. Ordaz and Pérez-Rocha proposed a new rule for estimating the SRF of elastoplastic SDOF systems, in which reduction factors are dependent only on displacement elastic spectra [12]. Chopra and Chintanapakdee evaluated the effects of near-fault with forward directivity characteristic and far-fault earthquakes on the SRF. They revealed that the near-fault records have a lower SRF than far-fault ground motions in the region of intermediate periods [13]. Miranda and Ruiz-Garcia investigated the effect of stiffness degradation on the lateral strength demands of inelastic SDOF systems subjected to 116 earthquake ground motions. It was concluded that in structures with stiffness degradation whose period of vibration is approximately equal to the predominant period of the earthquake, the SRF is smaller than the non-degrading structures [14]. Zahi and Xie investigated the effects of classification of design earthquake, soil condition, earthquake magnitude and distance to the rupturing fault on the SRF by analyzing 823 earthquakes records. They concluded that for higher ductility in short periods, the effect of soil condition cannot be ignored. Furthermore, they revealed that the classification of design earthquake has an important effect on the SRF for short-period systems, while the earthquake magnitude has a negligible influence [15]. Zhai et al. examined the effect of the near-fault pulse-like ground motions on the SRF. They showed that, in the range of short and medium periods, the SRF resulting from the near-fault pulse-like ground motions is less than that from the far-fault ground motions. Also, some modification factors for evaluating the SRF for the near- fault earthquakes were presented [16]. Gillie et al. studied the effect of pulse-type records by considering two earthquake groups, including 82 records with forward directivity (FD) effect and 63 records without forward directivity (Non-FD) effect. They found that the SRF of structures subjected to FD records, especially in the case of short periods and large ductility factors, is lower than Non-FD records [17]. In another research, the effect of near-fault earthquake records with directivity-induced pulses on the SRF was also investigated [18]. Zhai et al. carried out a study for evaluating the effect of mainshock–aftershock sequence-type ground motions, vibration period, ductility ratio, and hysteretic deterioration on the SRF. Their examinations showed that the effect of the aftershock on the SRF depends on the period of the structure, ductility level and the intensity of the aftershocks [19]. Zhang et al. investigated the SRF of SDOF systems under the effect of mainshock–aftershock sequences of ground motions and concluded that the damage-based SRF is about 0.6–0.9 times of the ductility-based SRF [20]. Poursha and Habibi studied the SRF based on ground motions recorded in Iran and proposed expressions for the SRF in terms of the period of a system and level of ductility by means of statistical analysis [21]. Dong et al. evaluated the SRF of self-centering structures with flag-shaped hysteretic behavior subjected to near-fault pulse-like earthquakes and proposed an equation for the SRF of this type structures [22]. In other investigations, the effects of soil-structure interaction [23], bi-directional seismic excitation [24], and the spectral shape of ground motion records, P-delta and cyclic deterioration [25] on the SRF were studied. A brief summary of the investigations implemented on the SRF, and the most important characteristic(s) considered in each research is presented in Table 1.

In the previous investigations, the SRF has been studied for near-fault records with forward-directivity characteristic and far-fault records. To the authors' knowledge, the influence of near-fault records with fling step effect and non-

pulse-like near-fault ground motions on the strength reduction factor has not been investigated in the previous studies; therefore, existing SRF equations can not be applied to this type of earthquake records. Moreover, the results from these four types of records have not been compared with together. In this paper, the strength reduction factor was studied for different types of ground motions including the pulse-like near-fault records with forward directivity and fling step effects and non-pulse-like near-fault and far-fault records. It is noted that forward-directivity and fling step effects can cause severe structural damage [26], but the characteristics of fling-step are different from forward-directivity. Forward-directivity has a two-sided velocity pulse, whereas fling-step effects cause a one-sided velocity pulse and a residual displacement at the end of the record [27]. Consequently, fling-step is considered by a discrete step in a displacement time-history of the ground motion record [28]. Fling-step is the effect of the permanent tectonic offset, caused by a rupturing fault, in near-fault ground motions [29]. In the current research, the effect of pulse period, ductility level and the cyclic deterioration on the SRF was studied by using the modified Ibarra-Medina-Krawinkler (the modified IMK) deterioration model [30]. Also, the merit of the current paper is that the results obtained in this study were compared to some equations proposed by other researchers in the previous investigations. Finally, by means of the nonlinear regression analysis performed on the results obtained, equations were individually presented for different types of seismic ground motions used.

2. Modeling of the SDOF system

For modeling and performing the linear and nonlinear analyses in OpenSees [31] program, a single degree of freedom oscillator with an inelastic spring is considered as shown in Fig. 1 [32-35]. The model is composed of an inverted pendulum of length, h, with the elastic material and a lumped mass, m, at the top of it. It is assumed that an inelastic rotational spring with the initial stiffness, K_r, supports the base of the rigid rod. It is supposed that the mass is constant and the change in the stiffness of the system produces different periods of vibration. To perform the time history analyses, the numerical direct integration scheme by means of the implicit Newark method with constant acceleration (i.e., $\gamma = 0.5$ and $\beta = 0.25$) [33] was used.

3. The modified Ibarra-Medina-Krawinkler hysteretic model

The Ibarra-Madina-Krawinkler (IMK) deterioration model was presented in 2005. This model can include three hysteretic models in a structure such as the bilinear model, peak-oriented model, and pinching model. Also, it was shown that four cyclic deterioration modes, including basic strength deterioration, post-capping deterioration, unloading stiffness degradation and accelerated reloading stiffness degradation can happen in cyclic loadings. It should be noted that the accelerated reloading stiffness degradation is not a deterioration mode for a component with bilinear hysteretic model [36]. The Ibarra-Madina-Krawinkler deterioration model was modified by Lignos [37] to be able to consider the component asymmetric hysteretic behavior including different rates of cyclic deterioration in two directions of loading and residual resistance.

In this paper, the modified Ibarra-Medina-Krawinkler model with bilinear hysteretic behavior was taken into consideration, as shown in Fig. 2 [30]. The parameters of the backbone curve of the modified IMK model with bilinear hysteretic behavior were calculated considering the ductility ratio (θ_c/θ_y), the strain hardening ratio for positive and negative directions (α_s), the post capping stiffness ratio (α_c) and zero residual moment ($M_r = 0$) by using the equations specified in Ref. [36]. It should be noted that this model can be used for any type of the force-displacement relationship, but the moment-rotation relationship is used in the present study.
The reference hysteretic energy dissipation capacity in the original IMK model is equal to:

$$E_t = F_y \times \delta_y \times \gamma_{s,c,k,a} \tag{2}$$

where $\gamma_s, \gamma_c, \gamma_k, \gamma_a$ represent the basic strength deterioration, post-capping deterioration, unloading stiffness degradation and accelerated reloading stiffness degradation, respectively. Connecting the hysteretic energy dissipation capacity to the yielding deformation, δ_y, is not a stable measure because the term, δ_y is affected by various factors. For this purpose, the stable factor of δ_p is used to define the hysterical energy dissipation capacity. Therefore, in the modified IMK model, the reference hysteretic energy dissipation capacity is equal to:

$$E_t = \lambda_{s,c,\mathrm{k},a} \times F_y \times \delta_p \tag{3}$$

in which $\lambda_s, \lambda_c, \lambda_k, \lambda_a$ are the rates of deterioration for four cyclic deterioration modes [37].
In this study, in order to achieve the elastoplastic state in the modified IMK model, the values of $\theta_c/\theta_y = \infty$, $\gamma = \infty$ and $\alpha_s = 0$ were considered. Also, to investigate the effect of cyclic deterioration on the strength reduction factor, the ratio of the ductility ratio was considered to be equal to $\theta_c/\theta_y = 4$, while the ratio of the residual strength was equal to zero. Moreover, the strain hardening ratio for the positive and negative directions was $\alpha_s = 0.03$. Also, α_c was equal to -0.2. The values of $\lambda_{s,c,k}$ were considered to be $\lambda_{s,c,k} = 3, 5, 10, 25, 50$ and 100 in which the lowest value of γ corresponds to the maximum deterioration level of the structure.

Strength reduction factors are strongly affected by the period of vibration. In this study, a sensitivity analysis was performed to examine the variation of $R_\mu$based on the period. Finally, 1324 periods were used in the range of 0.02 to 50 s. For the periods from 0.02 to 0.5, 0.52 to 20 and 20.1 to 50 s, the period intervals of 0.01, 0.02 and 0.1 s were used, respectively. Moreover, ductility demand ratios of 1.5, 4 and 6 were considered for evaluating the effect of ductility level on the SRF, while the damping ratio was assumed to be 5%.

4. Selection of ground motion records

The strength reduction factor (SRF) is strongly dependent on the type of the records selected; therefore, for different types of ground motion records, different results are obtained. In this paper, a comprehensive study was carried out for four categories of seismic records (see Table 2) [38]. The first category consists of 18 records showing the effect of fling step (FS) [39-43]. Each set of the other three groups contains 20 records with forward directivity effect (FD) [44], with no pulse (NP) [45-47], and far-fault (FF) [45] characteristics. More details of the seismic records are listed in Tables 3 to 6. All the records were from site C or D, based on the site classification in accordance with the NEHRP [48]. They were selected from the PEER (Pacific Earthquake Engineering Research) database. It should be noted that to obtain the R_μ value for each set of earthquake records, time history analyses were individually performed for each set; then, the mean of the R_μ values for each set was separately determined. Fig. 3 shows the flowchart of the calculation of R_μ for a selected record.

5. Results and Discussion

5.1 Strength reduction factor for elastoplastic system

At the long periods region, R_μ tends to μ; therefore, periods up to 50 s were used in this study. Fig. 4 shows the yield strength reduction factor spectrum for various ductility demand ratios of 1.5, 4, and 6 with 5% damping ratio. Fig. 4(a) represents that the SRF is almost equal for four seismic record sets with ductility demand ratio of $\mu = 1.5$ for periods shorter than 0.2 s and longer than 2 s. The effect of the record type is mostly observed in periods between 0.3 and 2 s in which the pulse-like records have smaller SRF values compared to far-fault and non-pulse records. By increasing the ductility demand ratio to $\mu = 4$ and 6, for periods less than 0.1 s, the SRF is approximately equal for all of the 4 record sets, as seen in Figs. 4(b) and 4(c). It is also notable that the value of SRF for records with fling step effect, within the periods of 0.1 to 0.2 s is about 20% smaller in comparison with the other sets. The pulse effect on the SRF value is noticeable for periods between 0.3 and 2 s. In fact, for these periods, the value of SRF for the records with fling step and forward directivity effects is equal and it is less than that from far-fault and non-pulse records. The records with fling step effect produce the minimum SRF for periods varying from 2 to 4 s (the period of mid- and high-rise structures). Moreover, for periods longer than 4 s, the record type has almost no effect on the SRF. Analysis of non-pulse and far-fault records indicates that the value of SRF is almost equal for these two record sets for all of the periods studied.
To better examine and understand the results of the four sets of the ground motions, the SRF spectra for all seismic records which are normalized to the SRF of the far-fault ground motions are shown in Fig. 5. According to the figure, the differences in the strength reduction factor for the near-fault non-pulse records are negligible comparing to the far-fault records for all ductility demand ratios. Moreover, as can be observed in Fig. 5(a), the differences in the strength reduction factor for pulse-like and far-fault records with the ductility demand ratio of $\mu = 1.5$ are almost less than 20% which can be neglected. It may also be seen that for the ductility demand ratios of $\mu = 4$ and 6, the SRF (R_μ) for the records with fling step effect is about 20 to 40% less than the R_μ of far-fault ground motions for periods of 0.15 to

4 s, as seen in Figs. 5(b) and 5(c). Therefore, if the equations of far-fault ground motions are used to estimate the R_μ for structures with periods between 0.15 and 4 s (medium- to long-period structures that cover most of the engineering structures) when they are affected by fling step effects, the results would be underestimated and the strength of the design cannot be assured. In this case, the underestimation error would be by 20 to 40%. Consequently, structures with periods between 0.15 and 4 s should be designed for smaller R_μ, or in other words, for greater yield strength, when they are affected by fling step ground motion records. This difference is negligible for other periods; therefore, the equations of the far-fault ground motions can be used to estimate the R_μ for periods other than 0.15 to 4 s. For records with forward directivity effect and for ductility demand ratios of $\mu = 4$ and 6, the R_μ is approximately 20 to 40% less than that for far-fault records at periods of 0.4 to 2 s. Previous studies demonstrated that for the same peak ground acceleration and duration of shaking, records with directivity pulses can produce much higher base shears and inter-storey drifts in comparison with a record does not have these pulses [49]; therefore, more strength should be provided for records with directivity pulses. Moreover, the R_μ for the records with forward directivity and fling step effects are almost equal for periods between 0.4 and 2 s.

5.2 Coefficient of variation (C0V)

For higher levels of ductility demand ratio, the SRF increases. It is important not only to study the effect of ductility demand ratio on the SRF mean values but also to evaluate the dispersion of this factor. The coefficient of variation (COV) can show the dispersion of R_μ which is defined as the ratio of the standard deviation to the mean value of the data. The COV is calculated according to the specified ductility demand ratio for each seismic record set at a given time period [1].

Fig. 6 displays the COV for the SRF with different ductility demand ratios of 1.5, 4 and 6. According to this figure, for all seismic groups and for all ductility demand ratios, the COV strongly depends on the structural period within periods less than 0.5 s. Moreover, the increase in the period would reduce the effect of the structural period on COV. Also, the increase in the ductility demand ratio raises the COV.

5.3 Analyzing the effect of the pulse period

The pulse period (T_p) is considered as one of the most important characteristics of near-fault ground motions with forward directivity effect. The pulse period is defined as the time it takes a full velocity or acceleration cycle to occur in the velocity or acceleration time history. In this study, as can be observed in Table 7, two groups of ground motions were selected to investigate the effect of T_p. The values of T_p for pulse-like ground motions, given in Tables 3 and 4, were extracted from the strong ground motion database of the Pacific Earthquake Engineering Research (PEER) center.

Fig. 7 shows the effect of T_p on the yield strength reduction factor for different ductility demand ratios. Figs. 7(a) and 7(d) represent that the influence of pulse period classification on R_μ for records with fling step and forward directivity effects and for a ductility demand ratio of 1.5 is insignificant. As can be seen in Figs. 7(b) and 7(c), in records with fling step effect, for ductility demand ratios of 4 and 6 and for periods shorter than 8 s, the SRF is small for records with longer pulse periods, except for periods varying from 1 to 4 s in which the pulse period has an inconsiderable effect on R_μ. For periods between 7 and 13 s, the records with longer pulse periods give a higher strength reduction factor. Furthermore, Figs. 7(e) and 7(f) illustrate that the pulse period has no effect on the R_μ for records with forward directivity effect, ductility demand ratios of 4 and 6, and periods less than 0.5 s. Moreover, records with longer pulse periods result in smaller SRFs for systems with periods of 0.5 to 5 s. On the contrary, the records produce larger SRFs for systems whose periods are between 5 and 20 s.

5.4 Analyzing the effect of strength deterioration and stiffness degradation on the strength reduction factor

Fig. 8 displays the effect of hysteretic degradation on the yield strength reduction factor for the damping ratio of 5 % and ductility demand ratios of $\mu = 1.5,\ 4$ and 6. According to Figs. 8(a, d, g and j), the strength deterioration and stiffness degradation has no effect on the SRF for structures with a lower ductility demand ratio ($\mu = 1.5$). For systems with periods between 0.15 to 2 s, having the maximum deterioration ($\gamma = 3$) and ductility demand ratio of $\mu = 4$, the R_μ, in the case of the records with fling step effect, is about 20 to 30% lower than non-deteriorating systems (see Fig. 8(b)). This difference would increase by up to 40% for the ductility demand ratio of $\mu = 6$ in periods between 0.15

and 8 s. For the forward directivity near-fault records, the difference of R_μ between deteriorating and non-deteriorating systems with ductility demand ratio of $\mu = 4$, is lower than 20% (see Fig. 8(e)). With the increase in the ductility demand ratio ($\mu = 6$), the R_μ, for systems with the maximum deterioration ($\gamma = 3$) is approximately 20 to 30% lower than that for the non-deteriorating systems in periods varying from 0.1 to 4 s (see Fig. 8(f)). According to Figs. 8(h) and 8(k), for far-fault and non-pulse records, in systems having periods of 0.1 to 1 s, ductility demand ratio of $\mu = 4$ and the largest deterioration ($\gamma = 3$), the R_μ is about 20 to 30% lower than that for non-deteriorating systems, while for ductility demand ratio of $\mu = 6$, this difference reaches about 20 to 40%, in the range of periods between 0.1 to 7 s. As a consequence, the increase in strength and stiffness degradation would reduce the yield strength reduction factor. This conclusion is in agreement with the results from References [7, 14, 50].

5.5 Effect of normalization of the system period with respect to the pulse period on the strength reduction factor

The effect of normalization of the system period in the case of forward directivity ground motion records has been shown in some previous investigations such as [13, 17, 51-53]. Fig. 9 displays the effect of normalization of the system period with respect to the pulse period on the strength reduction factor for pulse-like (fling-step and forward directivity) ground motions for the damping ratio of 5% and ductility demand ratios of $\mu = 1.5,\ 4$ and 6. According to the figure, for the small ductility ratio, normalization of the system period to the pulse period leads to a little difference on the strength reduction factor. With the increase in the ductility, it can be observed that a large difference appears in periods less than 4 seconds and the difference between the SRFs obtained for the normalized and non-normalized periods amounts to 60%. On the other hand, as shown in Figs. 9(a) and 9(b), at periods greater than 4 seconds, the strength reduction factor for the normalized periods is smaller than that for the non-normalized periods. This comparison indicates that the results obtained in this study are consistent with those from Reference [17].
In addition, by comparing the strength reduction factors obtained for the records with forward directivity and fling-step effects when the system period is normalized to the pulse period, no meaningful difference is observed for the lower ductility ($\mu = 1.5$), while with the increase in the ductility for the normalized periods less than 0.5, the strength reduction factor for the records with fling-step effect is approximately 20 to 30% larger than those with forward directivity effect, as seen in Fig. 9(c). They are approximately close together for normalized periods longer than 0.5 seconds.

6. Equations proposed for the yield strength reduction factor

Based on the results obtained in this study, equations were proposed to determine the yield strength reduction factor for different ground motion sets described earlier. To this end, the limit values are established for the SRF according to Table 8.
Considering the above-mentioned conditions, Eqs. 4 to 7 are proposed to determine the SRF for each seismic record set. It is assumed that the SRF is a function of the vibration period, the ductility demand ratio and the type of seismic excitation. For the purpose of curve fitting, a nonlinear least-squares regression analysis by means of the Levenberg-Marquardt algorithm was implemented in MATLAB [54] software. The following equations are presented for the yield strength reduction factor for different seismic record sets: For near-fault pulse-like records with fling step and forward directivity effects:

$$R_\mu = \left[1+(\mu-1)(\theta_1+\theta_2)e^{\left(\frac{1}{\mu}\right)}\left(1+e^{-\theta_1\left(\frac{1}{T-0.02}\right)^{0.5}}+(\mu-1)\theta_2 T^{0.6}-e^{-\theta_3 T^{0.8}}+\theta_4 T^2 e^{-\theta_5 T}\right)\right] \quad (4)$$

For near-fault non-pulse records:

$$R_\mu = \left[1+(\mu-1)(\theta_1+\theta_2)e^{\left(\frac{1}{\mu}\right)}\left(1+e^{-\theta_1\left(\frac{1}{T}\right)}+\mu\theta_2 T^{0.3}-e^{-\theta_3 T^{0.5}}+\theta_4 T^2 e^{-\theta_5 T}\right)\right] \quad (5)$$

For far-fault records:

$$R_\mu = \left[1+(\mu-1)\left(1-e^{-\theta_1 T^{1.25}}+\theta_2 T^{1.25} e^{-\theta_3 T}\right)\right] \quad (6)$$

$$\theta_{i=1,2,3,4,5} = P_{1,i}\mu^2 + P_{2,i}\mu + P_{3,i} \quad (7)$$

in which the parameters, θ_i, are the curve fitting constants. They are dependent on the ductility demand ratio and on the constants $P_{1,i}$, $P_{2,i}$ and $P_{3,i}$ and are calculated by using Eq. (7). In order to calculate θ_i, constants $P_{1,i}$, $P_{2,i}$ and $P_{3,i}$ are given in Table 9 for a specific type of ground motions. The strength reduction factors obtained from the time history analysis and from the proposed equations for different types of ground motion records are displayed in Fig. 10.

The coefficient of determination (R^2) is an indicator that shows how well the regression model fits the data. The coefficient R^2 is between 0 and 1. The value of 1 indicates that the predicted regression model is completely appropriate. Excellent fits generally have R^2 equal to or larger than 0.9 and fair to good fits have values between 0.7 and 0.9.

Moreover, the Root Mean Square Error (RMSE) is used, in this study, to show the differences between the predicted values from the fitted equation and the real values calculated. It calculates the average magnitude of the errors. The RMSE parameter can be derived from the following equation:

$$RMSE = \sqrt{\frac{1}{n}\sum\left(X_i - Y_i\right)^2} \quad (8)$$

where n is the number of data, X_i are the real data obtained from the analysis and Y_i are the values predicted from the fitting curve. If the RMSE tends to zero, the fitted curve would be ideal [55]. Table 10 illustrates that more excellent or better fits have been generally gained in this study for the ductility factors of 1.5 and 4 than $\mu = 6$. Also, the table demonstrates that in the case of ductility factors of 1.5 and 4, the values of RMSE for fling step records are larger than those for the other types of earthquake records. This means that the predictions are closer to the actual values in the case of FD, NP and FF records than FS records.

Fig. 11 displays a comparison of SRFs obtained in this work with those proposed earlier by the other researchers [1-2, 5-6, 10] for different ductility demand ratios of 1.5, 4, and 6 and for the damping ratio of 5%. Fig. 11(a) illustrates that, for the ductility demand ratio of 1.5, the SRFs obtained in this study for the four seismic record sets are similar to those from the proposed equations in the previous investigations to some extent. When the ductility demand ratio increases to $\mu = 4$ and 6, for periods between 0.15 to 4 s, the SRFs (R_μ) derived in the present study for the pulse-like records are about 20 to 40% less than those obtained in the previous studies, as can be observed in Figs. 11(b) and 11(c). Therefore, if the equations obtained in the previous investigations are used to estimate the R_μ for structures with periods between 0.15 and 4 s (that cover most of the engineering structures), the strength of the system will be underestimated for pulse-like (forward directivity and fling step) records and the design can not be assured. To generalize the results, a comprehensive study should be performed for pulse-like records considering other soil types, P-delta effects and other characteristics of near-fault ground motions.

Finally, it should be noted that the strength reduction factors obtained in this paper, are applicable to SDOF systems. Santa-Ana and Miranda showed that the strength reduction factor of Multi-Degree-of-Freedom (MDOF) systems is smaller than that of the corresponding SDOF ones whose natural periods are equal to the fundamental period of the MDOF buildings. Therefore, the lateral strength of MDOF systems is higher than that derived for SDOF ones [56].

7. Conclusions

In this paper, the SRF was investigated for different types of ground motions including the pulse-like near-fault records with forward directivity and fling step characteristics and non-pulse-like near-fault and far-fault records. The effect of the pulse period, ductility level and the cyclic deterioration on the SRF was studied by using the modified Ibarra-Medina-Krawinkler deterioration model. Also, the results obtained in this study were compared to some equations proposed by other researchers in the previous investigations. Finally, by means of the nonlinear regression analysis performed on the results obtained, equations were individually presented for different types of seismic ground motion records. The conclusions can be summarized as follow:

1. Investigating the effect of the vibration period and ductility demand ratio on the strength reduction factor reveals that the increase in the ductility demand ratio and the period would significantly raise the strength reduction factor. Furthermore, studying the pulse period of the four sets of ground motions reveals that the records with longer pulse periods would produce smaller values of R_μ compared to those with shorter pulse periods.
2. For a low ductility demand ratio, the type of seismic ground motion records would not have any influence on the strength reduction factor. Moreover, with the increase in the ductility demand ratio, the use of the equations proposed for far-fault ground motions underestimates the R_μ about 20 to 50% for near-fault records, especially for fling step records in the periods between 0.2 and 4 s. Therefore, structures which are affected by near-fault records with fling step effect should be designed for smaller values of R_μ or greater strength.
3. The results show that the increase in the ductility demand ratio would increase the effect of deterioration on the R_μ. Moreover, the increase in strength and stiffness degradation would reduce the yield strength reduction factor. Therefore, structures with strength and stiffness degradation should be designed for a greater strength force.
4. If the equations of the previous investigations (which were studied in this paper) are used to estimate R_μ for structures with periods between 0.15 and 4 s, the strength of the system would be underestimated for forward directivity and fling step records and the design can not be assured.
5. In this study, equations were proposed for the estimation of the yield strength reduction factor for the four sets of ground motions by using the nonlinear regression analysis. More excellent or better fits were obtained in this study for the ductility ratios of 4 and 6 in comparison with the ductility ratio of $\mu = 1.5$.

It is mentioned that the current investigation has some limitations in terms of some assumptions considered (e.g., only site classes C and D, particular magnitude of earthquakes, exclusion of P-delta effect). Another study is needed to address the mentioned limitations. Also, a comprehensive research is needed to study the SRF of MDOF systems. Research in this area continues.

Nomenclature

Parameter	
R_μ	Ductility-based Strength Reduction Factor due to Ductility
$K_{structure}$	Structure Stiffness (N/m)
f_o	Elastic Strength (N)
f_y	Yield Strength (N)
h	Rod Height
K_e	Initial Stiffness (N/m)
K_s	Hardening Stiffness (N/m)
K_c	Post-capping Stiffness (N/m)
T	Period (sec)
M_y	Yield Moment (N.m)
M_r	Residual Moment (N.m)
E_t	Reference Hysteretic Energy (N.m)
T_p	Pulse Period (sec)
$P_{1,i}$, $P_{2,i}$, $P_{3,i}$	Curve Fitting Constants
R^2	Coefficient of Determination
X_i	Real data obtained from the analysis
Y_i	The values predicted from the fitting curve
COV	Coefficient of Variation

Greek letters

μ	Ductility
α_s	Strain Hardening Ratio
α_c	Post Capping Stiffness Ratio
θ_y	Yield Rotation (rad)
κ	Residual Coefficient
θ_r	Residual Rotation (rad)
θ_{pc}	Post-capping Plastic Rotation (rad)
Δ_y , δ_y	Yield Deformation (cm)
δ_p	Plastic Deformation (cm)
γ_s	Basic Strength Deterioration
γ_c	Post-capping Deterioration
γ_k	Unloading Stiffness Degradation
γ_a	Accelerated Reloading Stiffness Degradation
$\lambda_s, \lambda_c, \lambda_k, \lambda_a$	Rates of Deterioration
φ	Rotation Angle (rad)
θ_y	Yield Rotation (rad)
θ_c	Capping Rotation (rad)
Δ_o	Maximum Elastic Deformation (cm)
θ_i	Curve Fitting Constants

Declaration of Competing Interest

The authors declare that they have no known competing financial interests or personal relationships that could have appeared to influence the work reported in this paper.

References

1. Miranda, E., Site-dependent strength-reduction factors. Journal of Structural Engineering, 1993. **119**(12).
2. Newmark, N.M. and W.J. Hall, Seismic design criteria for nuclear reactor facilities, in Proc of World Conf on Earthquake Engineering. 1973. p. 37-50.
3. Hidalgo, P.A. and A. Arias. New Chilean code for earthquake-resistant design of buildings. in Proceedings 4th US National Conference on Earthquake Engineering. 1990.
4. Lai, S.S. and J.M. Biggs, Inelastic response spectra for aseismic building design. Journal of the Structural Division, 1980. **106(6**: p. 1295-1310.
5. Riddell, R., P. Hidalgo, and E. Cruz, Response modification factors for earthquake resistant design of short period buildings. Earthquake Spectra, 1989. **5**(3): p. 571-590.
6. Riddell, R. and N.M. Newmark, Statistical analysis of the response of nonlinear systems subjected to earthquake. 1979: University of Illinois Engineering Experiment Station, College of Engineering, University of Illinois at Urbana-Champaign.
7. Al-Sulaimani, G.J. and J.M. Roessett, Design spectra for degrading systems. Journal of Structural Engineering, 1985. **111**(12): p. 2611-2623.
8. Elghadamsi, F.E. and B. Mohraz, Inelastic earthquake spectra. Earthquake Engineering & Structural Dynamics, 1987. **15**(1): p. 91-104.
9. Peng, M.H., F. Elghadamsi, and B. Mohraz. A stochastic procedure for nonlinear response spectra. in Ninth World Conference on Earthquake Engineering, Tokyo-Kyoto. 1988. Japan.
10. Nassar, A.A. and H. Krawinkler, Seismic demands for SDOF and MDOF systems. 1991: John A. Blume Earthquake Engineering Center, Department of Civil Engineering, Stanford University.
11. Miranda, E. and V.V. Bertero, Evaluation of structural response factors using ground motions recorded during the Loma Prieta earthquake. 1991.
12. Ordaz, M. and L. Pérez-Rocha, Estimation of strength-reduction factors for elastoplastic systems: a new approach. Earthquake engineering & structural dynamics, 1998. **27**(9): p. 889-901.

13. Chopra, A.K. and C. Chintanapakdee, Comparing response of SDF systems to near-fault and far-fault earthquake motions in the context of spectral regions. Earthquake Engineering & Structural Dynamics, 2001. **30**(12): p. 1769-1789.
14. Miranda, E. and J. Ruiz-Garcia, Influence of stiffness degradation on strength demands of structures built on soft soil sites. Engineering Structures, 2002. **24**(10): p. 1271-1281.
15. Zhai, C.H. and L. Xie, Study on strength reduction factors considering the effect of classification of design earthquake. Acta Seismologica Sinica, 2006. **19**(3): p. 299-310.
16. Zhai, C.H., H.B. Liu, and L.L. Xie. Near-fault Pulse-like Effect on Strength Reduction Factors. in 4th International Conference on Earthquake Engineering. 2006. Taipei: Taiwan.
17. Gillie, J.L., A. Rodriguez-Marek, and C. McDaniel, Strength reduction factors for near-fault forward-directivity ground motions. Engineering Structures, 2010. **32**(1): p. 273-285.
18. Qu, H., J. Zhang, and J. Zhao, Strength reduction factors for seismic analyses of buildings exposed to near-fault ground motions. Earthquake Engineering and Engineering Vibration, 2011. **10**(2): p. 195-209.
19. Zhai, C.H., et al., The ductility-based strength reduction factor for the mainshock–aftershock sequence-type ground motions. Bulletin of Earthquake Engineering, 2015. **13**(10): p. 2893-2914.
20. Zhang, Y., J. Chena, and C. Sun, Damage-based strength reduction factor for nonlinear structures subjected to sequence-type ground motions. Soil Dynamics and Earthquake Engineering, 2017. **92**: p. 298-311.
21. Poursha, M. and S. Habibi, Yield strength reduction factor and inelastic displacement ratio based on earthquake ground motions recorded in Iran. Journal of Civil and Environmental Engineering, 2019. **49**(3): p. 9-22.
22. Dong, H., et al., Strength reduction factor of self-centering structures under near-fault pulse-like ground motions. Advances in Structural Engineering, 2021. **24**(1): p. 119-133.
23. Anand, V. and S.R. Satish Kumar, Sensitivity of strength reduction factor for structures considering soil-structure interaction. Structures, 2022. **39**: p. 593-606.
24. Wang, F., et al., Damage-based strength reduction factor spectra of structures subjected to bidirectional ground motions, in Advances in Structural Engineering. 2023. p. 1-17.
25. Bohlouli, Z. and M. Poursha, Effects of P-delta and Spectral Shape of Ground Motion Records on Strength Reduction Factor and Inelastic Displacement Ratio of SDOF Systems with Deterioration. Structures, 2024. **69**: p. 107410-107410.
26. Hamidi, H., H. Khosravi, and R. Soleimani, Fling-step ground motions simulation using theoretical-based Green's function technique for structural analysis. Soil Dynamics and Earthquake Engineering, 2018. **115**: p. 232-245.
27. Stewart, J.P., et al., Ground motion evaluation procedures for performance-based design. 2002: Berkeley.
28. Bray, J.D. and A. Rodriguez-Marek, Characterization of forward-directivity ground motions in the near-fault region. Soil Dynamics and Earthquake Engineering, 2004. **24**(11): p. 815-828.
29. Kamai, R., N. Abrahamson, and R. Graves, Adding fling effects to processed ground-motion time histories. Bulletin of the Seismological Society of America, 2014. **104**(4): p. 1914-1929.
30. Ibarra, L.F., R.A. Medina, and H. Krawinkler, Hysteretic models that incorporate strength and stiffness deterioration. Earthquake Engineering and Structural Dynamics, 2005. **34**(12): p. 1489-1511.
31. OpenSees, Open system for earthquake engineering simulation. 1997, Berkeley, CA: Pacific Earthquake Engineering Research Center, University of California.
32. Adam, C. Global collapse capacity of earthquake excited multi-degree-of-freedom frame structures vulnerable to P-delta effects. in In proceedings of the Taiwan–Austria joint workshop on computational mechanics of materials and structures. 2008.
33. Chopra, A.K., Dynamics of Structures: Theory and Applications to Earthquake Engineering. 4th ed. 2020, Englewood Cliffs, New Jersey: Prentice Hall.
34. Norouzi, A. and M. Poursha, The collapse period of degrading SDOF systems considering a broad range of structural parameters. Soil Dynamics and Earthquake Engineering, 2018. **115**: p. 730-741.
35. Norouzi, A. and M. Poursha, Effect of the spectral shape of ground motion records on the collapse fragility assessment of degrading SDOF systems. Earthquake Engineering and Engineering Vibration, 2021. **20**: p. 925-941.
36. Ibarra, L.F. and H. Krawinkler, Global collapse of frame structures under seismic excitations. 2004, Berkeley, CA: Pacific Earthquake Engineering Research Center.
37. Lignos, D., Sidesway collapse of deteriorating structural systems under seismic excitations. 2008: Stanford University.

38. Motallebi, S.E., M. Poursha, and Z. Bohlouli, Inelastic displacement ratio for degrading SDOF systems under the Effect of pulse-like and non-pulse-like near-Fault ground motions. Journal of Civil and Environmental Engineering, 2024. **53**(4): p. 36-52.
39. A. Daei, M. Poursha, and M. Zarrin, Sensitivity of structural responses to the processing of near-fault ground motion records containing fling-step. Advances in Structural Engineering, 2023. **26**(6): p. 1114-1129.
40. Davoodi, M. and M. Sadjadi, Assessment of near-field and far-field strong ground motion effects on soil-structure SDOF system. International Journal of Civil Engineering, 2015. **13**(3): p. 153-166.
41. Kalkan, E. and Kunnath S.K, Effects of fling step and forward directivity on seismic response of buildings. Earthquake Spectra, 2006. **22**(2): p. 367-390.
42. Vafaei, D. and R. Eskandari, Seismic response of mega buckling-restrained braces subjected to fling-step and forward-directivity near-fault ground motions. The Structural Design of Tall and Special Buildings, 2015. **24**(9): p. 672-686.
43. Yang, D., J. Pan, and G. Li, Interstory drift ratio of building structures subjected to near-fault ground motions based on generalized drift spectral analysis. Soil dynamics and earthquake engineering, 2010. **30**(11): p. 1182-1197.
44. Shahi, S. and J. Baker, Pulse classifications from NGA West2 database. Np, 2012.
45. Federal Emergency Management Agency (FEMA) FEMA P695. 2009: Redwood City.
46. Li, S., et al., Effects of near-fault motions and artificial pulse-type ground motions on super-span cable-stayed bridge systems. Journal of Bridge Engineering, 2017. **22**(3): p. 4016128-4016128.
47. Song, J. and A. Rodriguez-Marek, Sliding displacement of flexible earth slopes subject to near-fault ground motions. Journal of Geotechnical and Geoenvironmental Engineering, 2015. **141**(3): p. 4014110-4014110.
48. Building Seismic Safety Council (BSSC). NEHRP recommended provisions for seismic regulations for new buildings and other structures. 2004, Washington (DC: FEMA-450.
49. Praveen, K.M., Response of buildings to near-field pulse-like ground motions. Earthquake Engineering and Structural Dynamics, 1999. **28**: p. 1309-1326.
50. Lee, L.H., S.W. Han, and Y.H. Oh, Determination of ductility factor considering different hysteretic models. Earthquake engineering and Structural Dynamics, 1999. **28**(9): p. 957-977.
51. Chioccarelli, E. and I. Iervolino, Near-Source seismic demand and pulse-like records", a Discussion for L'Aquila Earthquake. Earthquake Engineering and Structural Dynamics, 2010. **39**(9): p. 1039-1062.
52. Iervolino, I., E. Chioccarelli, and G. Baltzopoulos, Inelastic displacement ratio of near-source pulse-like ground motions. Earthquake Engineering and Structural Dynamics, 2012. **41**: p. 2351-2357.
53. Ruiz-García, J., Inelastic Displacement Ratios for Seismic Assessment of Structures Subjected to Forward-Directivity Near-Fault Ground Motions. Journal of Earthquake Engineering, 2011. **15**(3): p. 449-468.
54. Matlab, The MathWorks, Inc. 1996, Online: Available.
55. Khoshnoudian, F., E. Ahmadi, and F.A. Nik, Inelastic displacement ratios for soil-structure systems. Engineering Structures, 2013. **57**: p. 453-464.
56. Santa-Ana, P.R. and E. Miranda. Strength reduction factors for multi-degree-of-freedom systems. in 12th World Conference on Earthquake Engineering. 2000. Auckland, New Zeland.
57. Mavroeidis, G.P., G. Dong, and A.S. Papageorgiou, Near-fault ground motions, and the response of elastic And inelastic single-degree-of-freedom (SDOF) systems. Earthquake Engineering and Structural Dynamics, 2004. **33**: p. 1023 49-1023 49.
58. Chakraborti, A. and V.K. Gupta, Scaling of strength reduction factors for degrading elasto-plastic oscillators. Earthquake Engineering and Structural Dynamics, 2005. **34**: p. 189-206.

Funding Declartion
The authors declare that no funds, grants, or other support were received during the preparation of this manuscript.

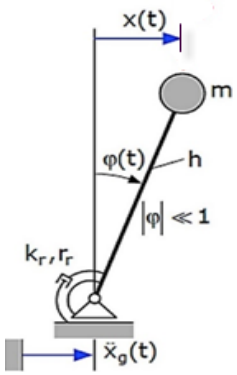

Fig. 1. The SDOF system considered in this study [28-30].

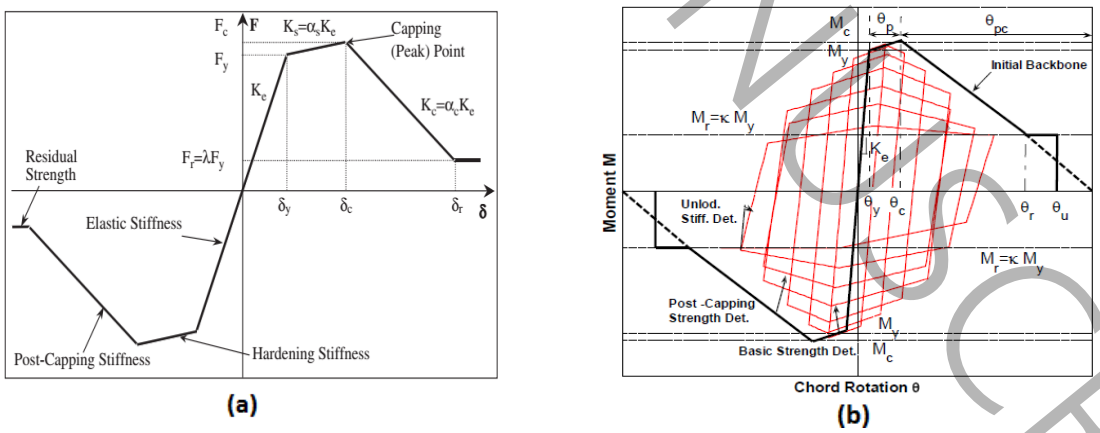

Fig. 2. a) The backbone curve for hysteretic models [26]; and b) the backbone curve for modified IMK model in OpenSees software [27]

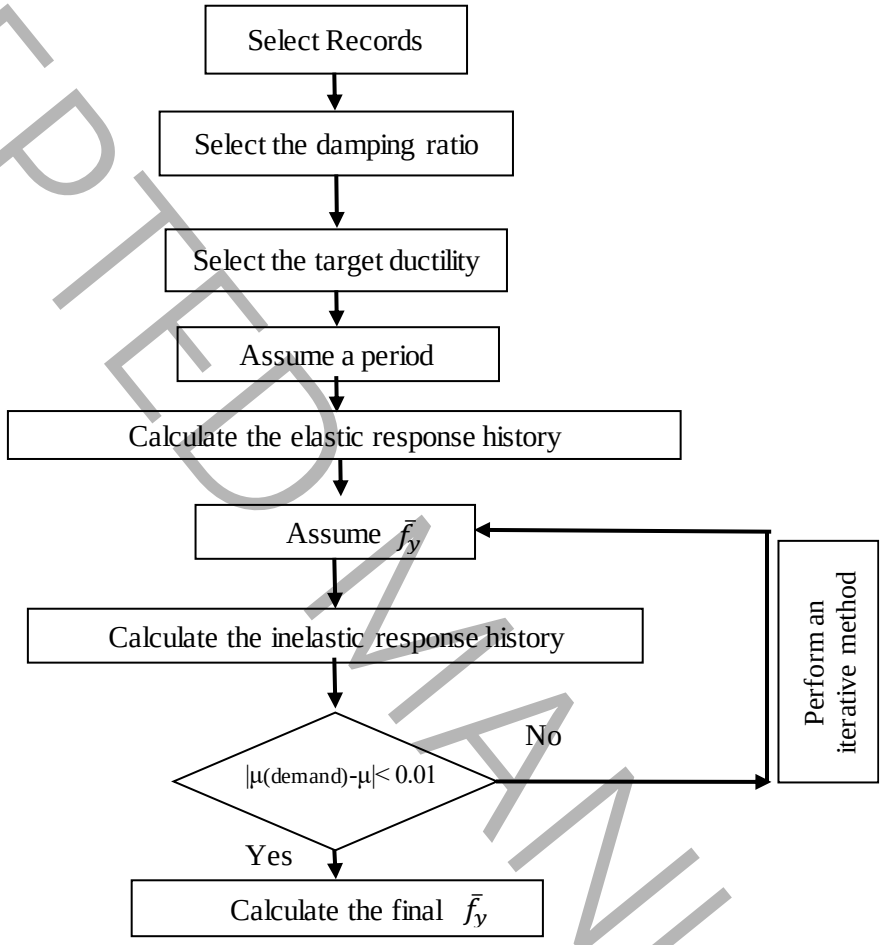

Fig. 3. Flowchart of the method for the calculation of the strength reduction factor due to ductility in SDOF systems [25].

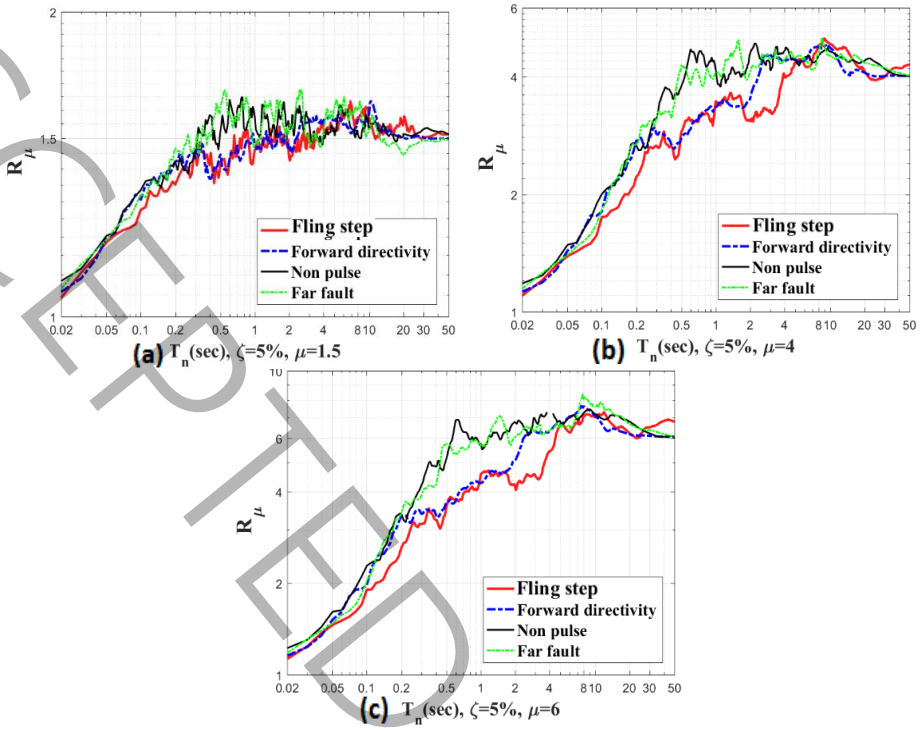

Fig. 4. The strength reduction factor of SDOF systems subjected to different sets of the ground motions for: a) $\boldsymbol{\mu = 1.5}$; b) $\boldsymbol{\mu = 4}$; and c) $\boldsymbol{\mu = 6}$

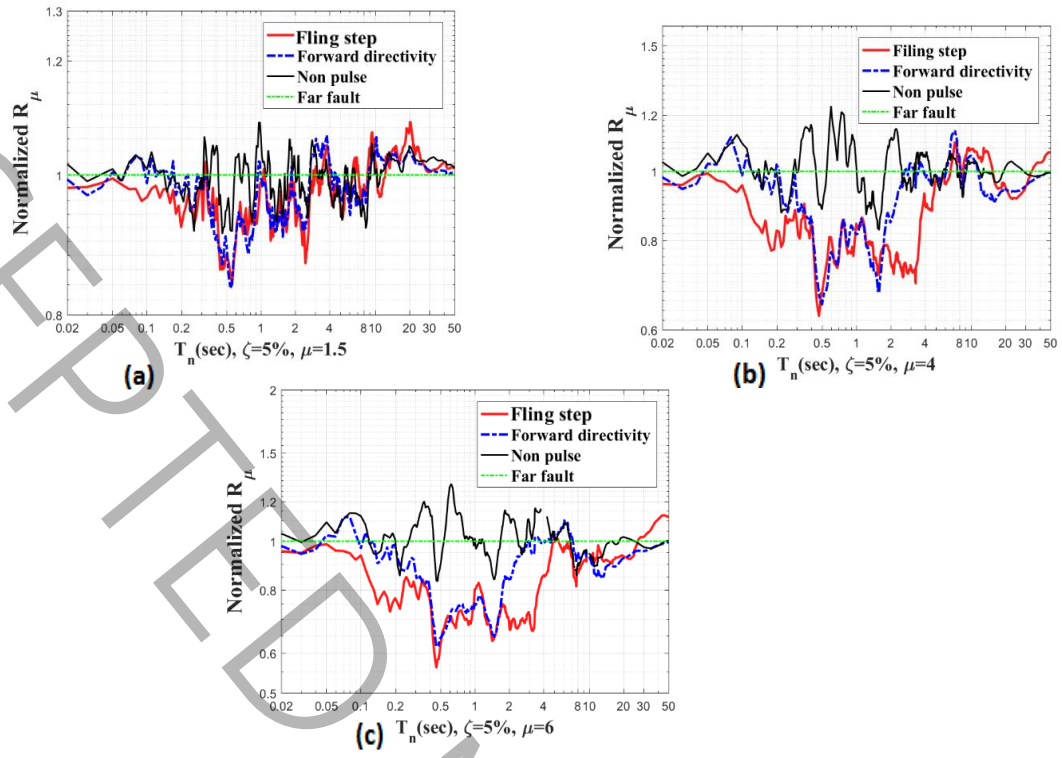

Fig. 5. The strength reduction factor of SDOF systems subjected to the four sets of the ground motions normalized to that from the far-fault ground motion set for ductility demand ratios of: a) $\boldsymbol{\mu = 1.5}$; b) $\boldsymbol{\mu = 4}$; and c) $\boldsymbol{\mu = 6}$

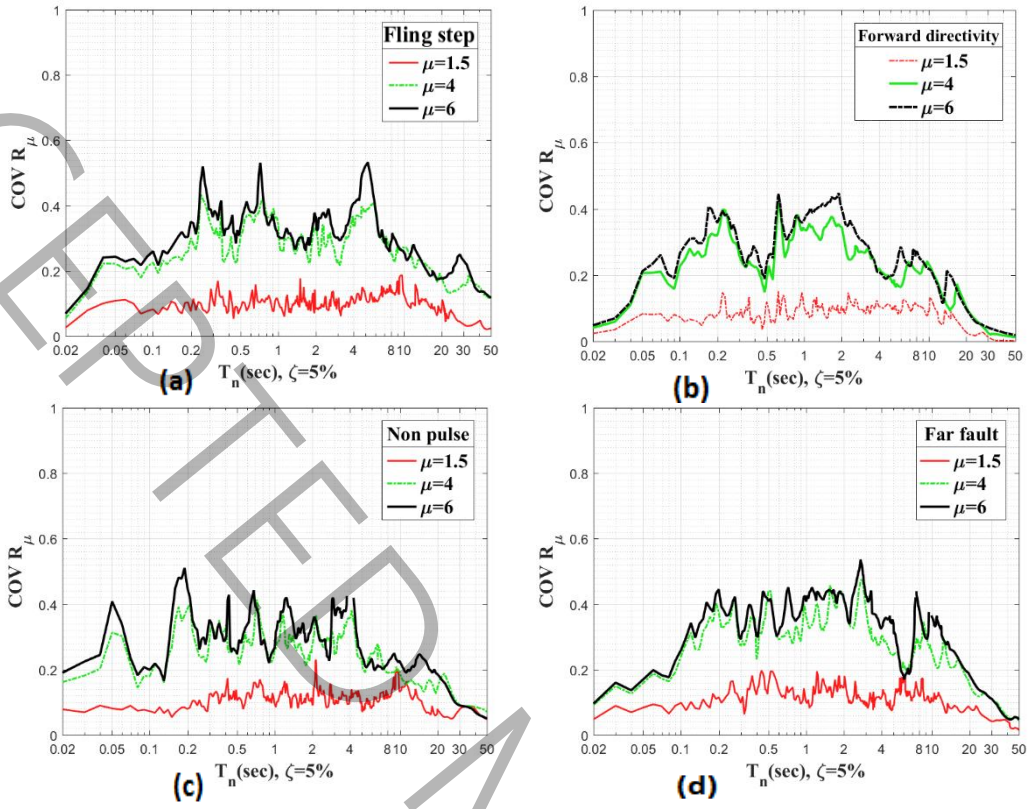

Fig. 6. The effect of ductility level on the dispersion of the strength reduction factor for SDOF systems subjected to near-fault and far-fault ground motions: a) Fling step; b) Forward directivity; c) Non pulse; and d) Far-fault

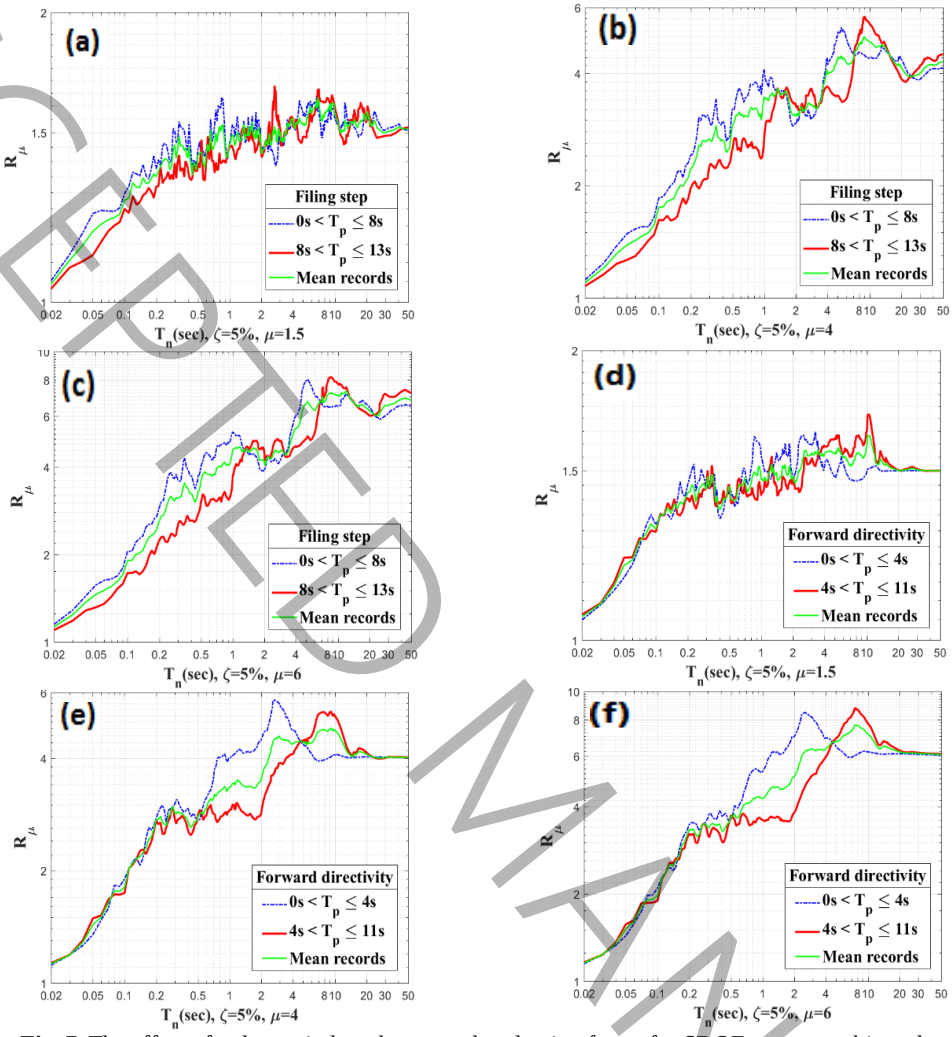

Fig. **7**. The effect of pulse period on the strength reduction factor for SDOF systems subjected to: (a-c) the near-fault records with filing step effect for $\boldsymbol{\mu = 1.5}$, **4**, and **6** ; and (d-f) the near-fault records with forward directivity effect for $\boldsymbol{\mu = 1.5}$, **4**, and **6**

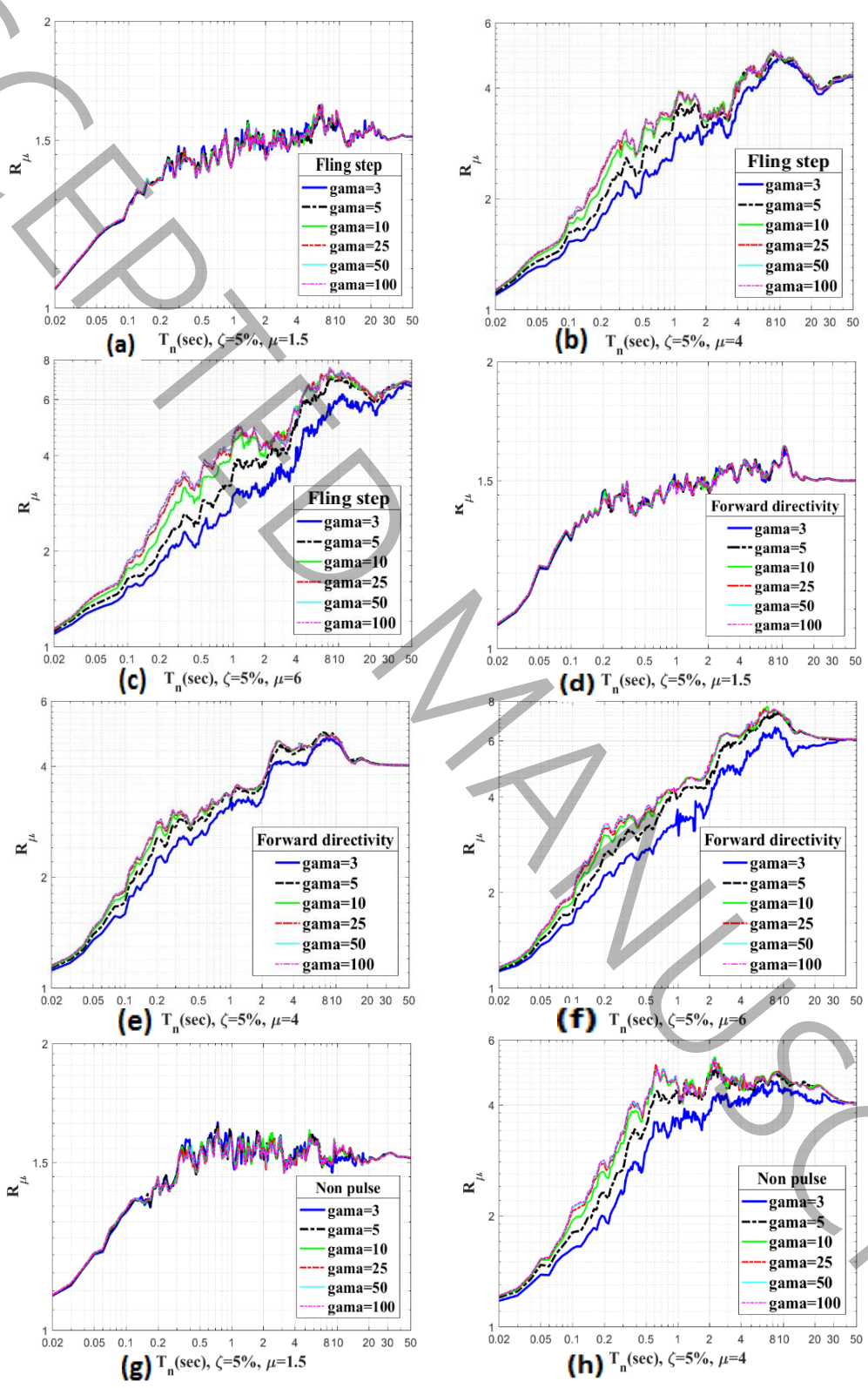

Fig. 8. The effect of strength deterioration and stiffness degradation on the strength reduction factor for SDOF systems subjected to the: (a-c) fling step records; (d-f) forward directivity records for ductility demand ratios of $\boldsymbol{\mu = 1.5}$, **4** and **6**; (g and h) non-pulse records for $\boldsymbol{\mu = 1.5}$ and **4**.

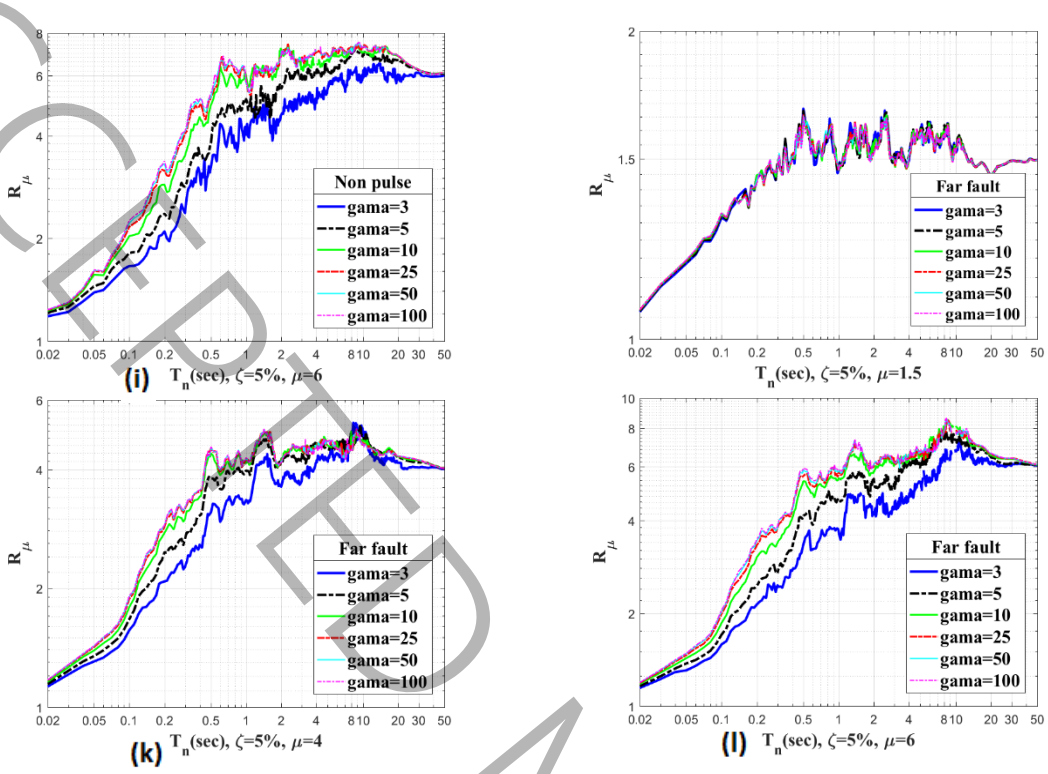

(i) (k) (l)

Fig. 8 (continued): (i) non-pulse records for ductility demand ratios of **6** ; and (j-l) far-fault records for $\boldsymbol{\mu} =$ **1**. **5**, **4** and **6**.

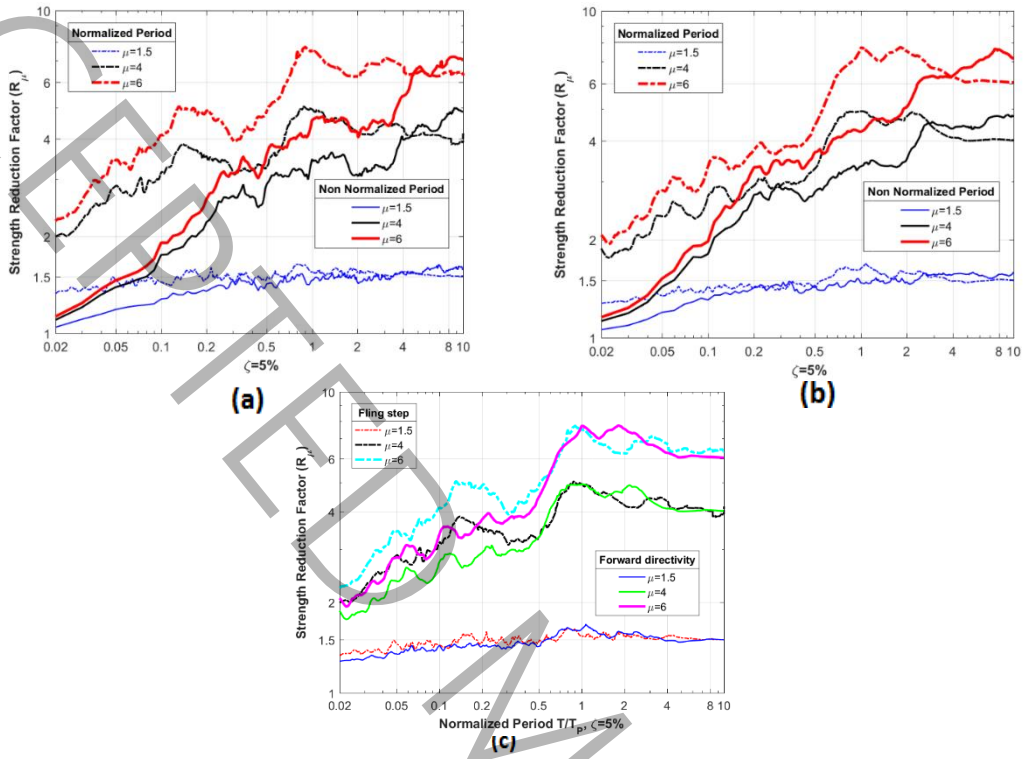

Fig. 9. Strength reduction factor for SDOF systems subjected to the: (a) fling step records with normalized period and non-normalized period; (b) forward directivity records with normalized period and non-normalized period; and (c) fling step and forward directivity records with normalized period

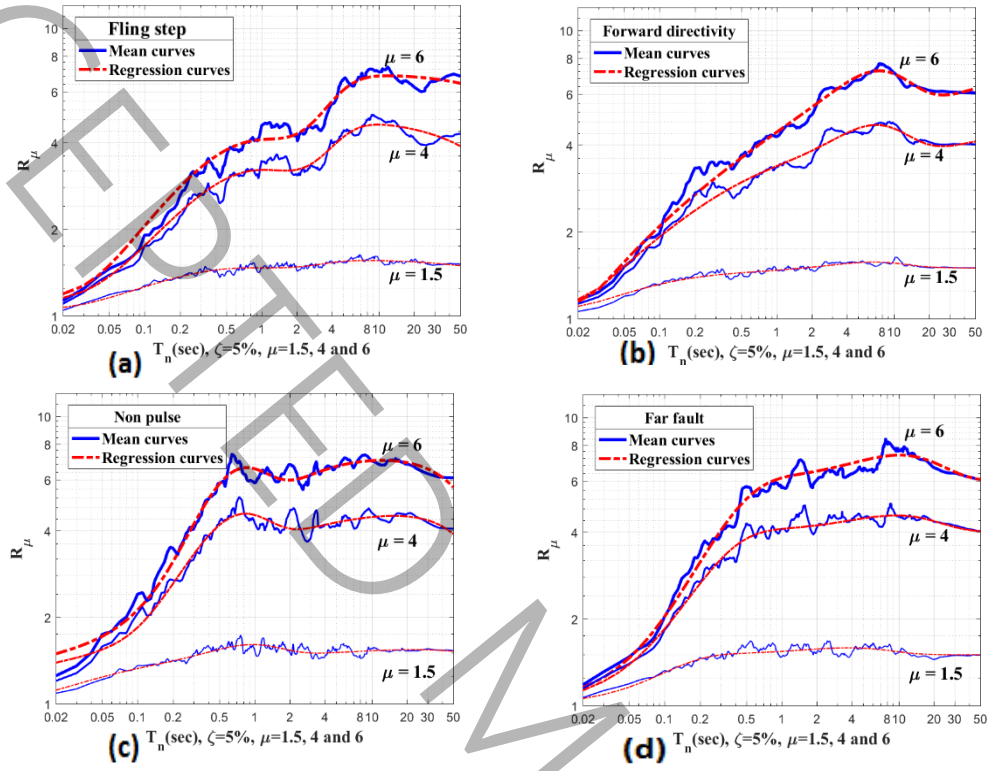

Fig. 10. The strength reduction factor obtained from the time history analysis and from the proposed equations (regression analysis) for: a) near-fault records with fling step effect; b) near-fault records with forward directivity effect; c) near-fault records without pulse (Non pulse); and d) far-fault records

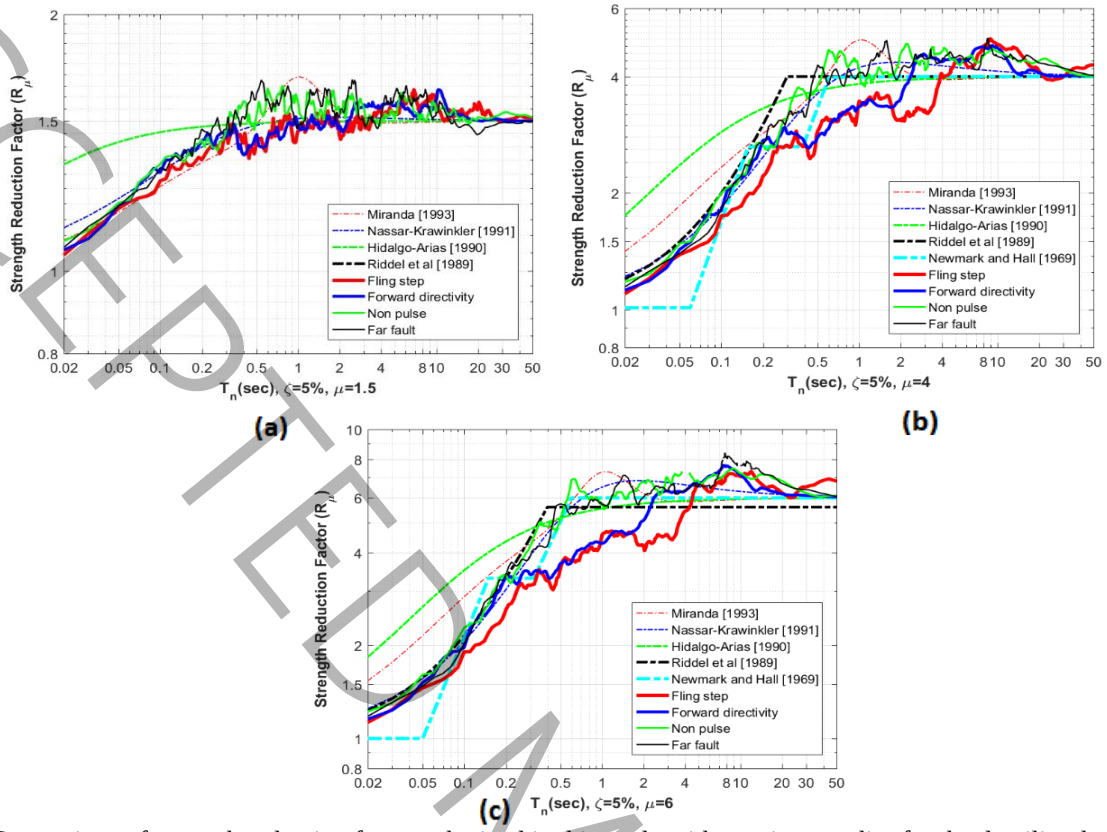

Fig. 11. Comparison of strength reduction factors obtained in this study with previous studies for the ductility demand ratios of: (a) $\boldsymbol{\mu = 1.5}$; (b) $\boldsymbol{\mu = 4}$ and (c) $\boldsymbol{\mu = 6}$.

Table 1. A brief summary of the investigations implemented on the SRF and the most important characteristic(s) considered in each research

Literature	The most important characteristic(s) considered (progress with respect to the previous studies)
Newmark and Hall 1969 [2]	Ductility and period
Al-Sulaimani and Roessett 1985 [7]	Stiffness and strength degradation
Elghadamsi and Mohraz 1987 [8]	Soil type
Peng et al. 1988 [9]	Duration of ground motions and damping ratio
Nassar and Krawinkler 1991 [10]	Epicentral distance, strain hardening and hysteretic model
Miranda and Bertero 1991 [11]	Soil type
Miranda 1993 [1]	Earthquake magnitude and epicentral distance
Chopra and Chintanapakdee 2001 [13]	Comparison of near-fault and far-fault earthquakes
Miranda and Ruiz-Garcia 2002 [14]	Stiffness degradation
Mavroeidis et al. 2004 [57]	Pulse of near-fault records
Chakraborti and Gupta 2005 [58]	Degradation of the system
Zhai and Xie 2006 [15]	Classification of design earthquake
Zhai et al. 2006 [16]	Pulse-like near-fault records
Gillie et al. 2010 [17]	Near-fault forward-directivity records
Zhai et al. 2015 [19]	Mainshock–aftershock sequence-type ground motions
Zhang et al. 2017 [20]	Damage-based SRF for sequence-type of ground motions
Poursha & Habibi, 2019 [21]	Ground motions recorded on the soft soil and rock site in Iran
Dong et al. 2021 [22]	Self-centering systems with flag-shaped hysteretic model
Anand and Kumar 2022 [23]	Soil-structure interaction
Wang et al. 2022 [24]	Bi-directional seismic excitation
Bohlouli and Poursha 2024 [25]	Spectral shape of ground motion records and P-delta effect

Table 2. Types of ground motion records used in this study

Types of ground motion records	Number of records in each ensemble
Fling step (FS) near-fault records	18
Forward-directivity (FD) near-fault records	20
Near-fault records with no pulse (NP)	20
Far-fault (FF) records	20

Table 3. Near-fault ground motions with fling step effect

No	Sequence Number	Earthquake name	year	Station name-comp	Magnitude	R_{rup} (km)	V_{s30} (m/s)	T_p	PGA (g)
1	1503	Chi-Chi, Taiwan	1999	TCU065-EW	7.62	0.57	305.85	5.74	0.78
2	1492	Chi-Chi, Taiwan	1999	TCU052-NS	7.62	0.66	579.10	11.95	0.44
3	1492	Chi-Chi, Taiwan	1999	TCU052-EW	7.62	0.66	579.10	11.95	0.35
4	1505	Chi-Chi, Taiwan	1999	TCU068-EW	7.62	0.32	487.34	12.28	0.51
5	1505	Chi-Chi, Taiwan	1999	TCU068-NS	7.62	0.32	487.34	12.28	0.37
6	1507	Chi-Chi, Taiwan	1999	TCU071-NS	7.62	5.80	624.85	6.41	0.65
7	1507	Chi-Chi, Taiwan	1999	TCU071-EW	7.62	5.80	624.85	7.17	0.52
8	1504	Chi-Chi, Taiwan	1999	TCU067-EW	7.62	0.62	433.63	5.25	0.49
9	1510	Chi-Chi, Taiwan	1999	TCU075-EW	7.62	0.89	573.02	4.99	0.33
10	1511	Chi-Chi, Taiwan	1999	TCU076-EW	7.62	2.74	614.98	4.73	0.34
11	1519	Chi-Chi, Taiwan	1999	TCU087-NS	7.62	6.98	538.69	10.39	0.11
12	1548	Chi-Chi, Taiwan	1999	TCU128-EW	7.62	13.3	599.64	9.02	0.14
13	1549	Chi-Chi, Taiwan	1999	TCU129-EW	7.62	1.83	511.18	5.17	1.00
14	1529	Chi-Chi, Taiwan	1999	TCU102-EW	7.62	1.49	714.27	9.63	0.30
15	1489	Chi-Chi, Taiwan	1999	TCU049-EW	7.62	3.76	487.27	10.22	0.27
16	1508	Chi-Chi, Taiwan	1999	TCU072-EW	7.62	7.08	468.14	5.51	0.47
17	1515	Chi-Chi, Taiwan	1999	TCU082-EW	7.62	5.16	472.81	8.09	0.22
18	1176	Kocaeli, Turkey	1999	Yarimca/YPT060	7.51	4.83	297.00	4.94	0.22

Table 4. Near-fault ground motions with forward directivity effect

No	Sequence Number	Earthquake name	year	Station name	Comp	Magnitude	R_{rup} (km)	V_{s30} (m/s)	T_p	PGA (g)
1	292	Irpinia, Italy-01	1980	Sturno (STN)	STU270.AT2	6.9	10.80	382	3.27	0.32
2	150	Coyote Lake	1979	Gilroy Array #6	G06230.AT2	5.7	3.10	663	1.23	0.42
3	459	Morgan Hill	1984	Gilroy Array #6	G06090.AT2	6.2	9.90	663	1.23	0.29
4	983	Northridge-01	1994	Jensen Filter Plant Generator	JGB022.AT2	6.7	5.40	526	3.54	0.57
5	4065	Parkfield-02, CA	2004	Parkfield – Eades	Eades360.AT2	6.0	2.90	384	1.22	0.39
6	6928	Darfield, New Zealand	2010	LPCC	Lpccs10e.AT2	7.0	25.70	660	10.63	0.35
7	1086	Northridge-01	1994	Sylmar - Olive View Med FF	Syl360.AT2	6.7	5.30	441	2.44	0.84
8	1148	Kocaeli, Turkey	1999	Arcelik	Are090.AT2	7.5	13.50	523	7.79	0.13
9	149	Coyote Lake	1979	Gilroy Array #4	G04360.AT2	5.7	5.70	222	1.35	0.25
10	161	Imperial Valley-06	1979	Brawley Airport	Bra225.AT2	6.5	10.40	209	4.40	0.16
11	170	Imperial Valley-06	1979	EC County Center FF	Ecc092.AT2	6.5	7.30	192	4.42	0.23
12	173	Imperial Valley-06	1979	El Centro Array #10	He10050.AT2	6.5	8.60	203	4.52	0.17
13	179	Imperial Valley-06	1979	El Centro Array #4	H04230.AT2	6.5	7.00	209	4.79	0.37
14	180	Imperial Valley-06	1979	El Centro Array #5	E05230.AT2	6.5	4.00	206	4.13	0.38
15	316	Westmorland	1981	Parachute Test Site	Pts225.AT2	5.9	16.70	349	4.39	0.23
16	182	Imperial Valley-06	1979	El Centro Array #7	E07230.AT2	6.5	0.60	211	4.38	0.46
17	184	Imperial Valley-06	1979	El Centro Differential Array	Eda270.AT2	6.5	5.10	202	6.27	0.35
18	185	Imperial Valley-06	1979	Holtville Post Office	Hvp225.AT2	6.5	7.50	203	4.82	0.25
19	568	San Salvador	1986	Geotech Investig Center	Gic090.AT2	5.8	6.30	330	0.81	0.70
20	900	Landers	1992	Yermo Fire Station	Yer270.AT2	7.3	23.60	354	7.50	0.24

Table 5. Near-fault ground motions without pulse

No	Sequence Number	Earthquake name	year	Station name	Comp.	Magnitude	R_{rup} (km)	$\mathbf{V_{s30}}$ $(\mathbf{m/s})$	PGA (g)
1	71	San Fernando	1971	Lake Hughes #12	L12021	6.61	19.30	602.00	0.382
2	160	Imperial Valley-06	1979	Bonds Corner	BCR-230	6.53	2.66	223.03	0.776
3	165	Imperial Valley-06	1979	Chihuahua	CHI-012	6.53	7.29	242.05	0.269
4	495	Nahanni, Canada	1985	Site 1	S1280	6.76	9.60	605.04	1.200
5	496	Nahanni, Canada	1985	Site 2	S2240	6.76	4.93	605.04	0.519
6	741	Loma Prieta	1989	BRAN	BRN090	6.93	10.72	476.54	0.502
7	753	Loma Prieta	1989	Corralitos	CLS0000	6.93	3.85	462.24	0.644
8	850	Landers	1992	Desert Hot Spring	DSP000	7.28	21.78	359.00	0.171
9	988	Northridge-01	1994	LA-Century City CC North	CCN090	6.69	23.41	277.98	0.255
10	1048	Northridge-01	1994	Northridge-17645Saticoy St	STC180	6.69	12.09	280.86	0.459
11	1205	Chi-Chi, Taiwan	1999	CHY041	EW	7.62	19.37	492.26	0.302
12	1504	Chi-Chi, Taiwan	1999	TCU067	EW	7.62	0.62	433.00	0.498
13	1513	Chi-Chi, Taiwan	1999	TCU079	EW	7.62	10.97	363.99	0.592
14	1533	Chi-Chi, Taiwan	1999	TCU106	EW	7.62	14.97	451.37	0.16
15	162	Imperial Valley	1979	Calexico Fire	CXO225	6.53	10.45	231.23	0.276
16	1080	Northridge-01	1994	Katherine Rd	KAT090	6.69	13.42	557.42	0.535
17	1087	Northridge-01	1994	Tarzana	TAR360	6.69	15.60	257.21	0.990
18	457	Morgan Hill	1984	Gilroy Array #3	GO3090	6.19	13.02	349.85	0.201
19	727	Super station Hills-02	1987	Super station Mtn Camera	SUP-135	6.54	5.61	362.38	0.837
20	959	Northridge-01	1994	Canoga park –Topanga Can	CNP196	6.69	14.70	267.49	0.391

Table 6. Far-fault ground motions

No	Sequence Number	Earthquake name	year	Station name	Comp.	Magnitude	R_{rup} (km)	Vs30 (m/s)	PGA (g)
1	68	San Fernando	1971	LA –Holly wood Stor FF	PEL090	6.61	22.77	316.46	0.22
2	125	Friuli, Italy-01	1976	LA – Holly wood Stor FF	TMZ000	6.50	15.82	505.23	0.35
3	169	Imperial Valley-06	1979	Delta	DLT352	6.53	22.03	242.05	0.34
4	174	Imperial Valley-06	1979	El Centro Array #11	HII230	6.53	12.56	196.25	0.37
5	721	Superstition Hills-02	1987	El Centro Imp. Co. Cent	ICC000	6.54	18.20	192.05	0.35
6	725	Superstition Hills-02	1987	Poe Road (temp)	POE270	6.54	11.16	316.64	0.47
7	752	Loma Prieta	1989	Capitola	CAP000	6.93	15.23	288.62	0.51
8	767	Loma Prieta	1989	Gilroy Array #3	GO3000	6.93	12.82	349.85	0.55
9	848	Landers	1992	Cool water	CLW-TR	7.28	19.74	352.98	0.41
10	900	Landers	1992	Yermo Fire Station	YER270	7.28	23.62	353.63	0.24
11	953	Northridge-01	1994	Beverly Hills - 14145 Mulhol	MUL279	6.69	17.15	355.81	0.48
12	960	Northridge-01	1994	Canyon Country - W Lost Cany	LOS270	6.69	12.44	325.60	0.47
13	1111	Kobe, Japan	1995	Nishi-Akashi	NIS000	6.90	7.08	609.00	0.48
14	1116	Kobe, Japan	1995	Shin-Osaka	SHI090	6.90	19.15	256.00	0.23
15	1148	Kocaeli, Turkey	1999	Arcelik	ARE000	7.51	13.49	523.00	0.21
16	1244	Chi-Chi, Taiwan	1999	CHY101	CHY101-N	7.62	9.94	258.89	0.39
17	1485	Chi-Chi, Taiwan	1999	TCU045	TCU045-N	7.62	26.00	704.64	0.50
18	1602	Duzce, Turkey	1999	Bolu	BOL090	7.14	12.04	293.57	0.80
19	1633	Manjil, Iran	1990	Abbar	ABBAR_L	7.37	12.55	723.95	0.51
20	1787	Hector Mine	1999	Hector	HEC090	7.13	11.66	723.95	0.32

Table 7. Characteristics of the groups of the ground motions classified according to the pulse period

Classification type	Record type	First group	Second group
Pulse period	**Fling Step**	$0 < T_p \leq 8\ s$	$8\ s \leq T_p < 13\ s$
	Forward directivity	$0 < T_p \leq 4\ s$	$4\ s \leq T_p < 11\ s$

Table 8. The limit values of the yield strength reduction factor

Period range	R_μ
Very short periods	$R_\mu \cong 1$
Long periods	$R_\mu = \mu$

Table 9. Values of constants $P_{1,i}$, $P_{2,i}$ and $P_{3,i}$

Fling step	θ_i	$P_{1,i}$	$P_{2,i}$	$P_{3,i}$
$i = 1$	θ_1	-0.02346	0.21475	0.14166
$i = 2$	θ_2	-0.00351	0.04271	-0.13266
$i = 3$	θ_3	0.30528	-3.21294	9.67952
$i = 4$	θ_4	0.01124	-0.17981	-0.29668
$i = 5$	θ_5	0.02918	-0.26525	1.50672
Forward directivity		$P_{1,i}$	$P_{2,i}$	$P_{3,i}$
$i = 1$	θ_1	-0.00179	0.02498	0.25646
$i = 2$	θ_2	-0.00296	0.02854	-0.053546
$i = 3$	θ_3	0.55646	-6.30562	19.28209
$i = 4$	θ_4	-0.00765	0.07289	-0.04272
$i = 5$	θ_5	-0.00096	0.002172	0.31110
Non pulse		$P_{1,i}$	$P_{2,i}$	$P_{3,i}$
$i = 1$	θ_1	0.02371	-0.01401	-0.00113
$i = 2$	θ_2	-0.00090	-0.04905	0.38690
$i = 3$	θ_3	0.00806	-0.06433	-0.01614
$i = 4$	θ_4	-0.78951	7.38351	-4.41886
$i = 5$	θ_5	-0.04780	0.57190	1.57830
Far fault		$P_{1,i}$	$P_{2,i}$	$P_{3,i}$
$i = 1$	θ_1	0.7173	-8.0510	26.5510
$i = 2$	θ_2	0.0081	-0.0747	0.2082
$i = 3$	θ_3	0.0169	-0.1735	0.5551

Table 10. Values of $\mathbf{R^2}$ and RMSE for the proposed equations

	$\mu = 6$		$\mu = 4$		$\mu = 1.5$	
Error measure	R^2	$RMSE$	R^2	$RMSE$	R^2	$RMSE$
Fling step	0.7577	0.0253	0.8680	0.2173	0.9078	0.3273
Forward directivity	0.7864	0.0225	0.9156	0.1422	0.9583	0.1910
Non pulse	0.4418	0.0351	0.8065	0.1710	0.9114	0.2158
Far fault	0.6114	0.0389	0.8743	0.1395	0.8644	0.3376